Supporting Information

Paulose et al. 10.1073/pnas.1212268109

SI Text

Fields and Strains in Shallow Shell Theory. We describe the deformations of the sphere, using shallow shell theory, which we summarize here. We follow the presentation by Koiter and van der Heijden (1). A shallow section of the sphere is isolated and Cartesian coordinates (x_1,x_2) are set up to define a plane that just touches the undeformed sphere at the origin and lies tangent to it; the z axis is thus normal to the sphere at the origin (Fig. S1). We use the Monge representation to parameterize the undeformed shell by its height $z = Z(x_1,x_2)$ above the plane, where $Z(x_1,x_2)$ is the undeformed state corresponding to a sphere of radius R with its center located on the z axis above the (x_1,x_2) plane:

$$Z(x_1,x_2) = R\left(1-\sqrt{1-\frac{x_1^2}{R^2}-\frac{x_2^2}{R^2}}\right). \quad [S1]$$

The assumption in shallow shell theory is that the section of the shell under consideration is small enough that slopes $\partial_1 Z \sim x_1/R$ and $\partial_2 Z \sim x_2/R$ measured relative to the (x_1,x_2) plane are small. (Partial derivatives are denoted by $\partial/\partial x_i \equiv \partial_i$.) Then the undeformed state is approximately parabolic in x_1 and x_2,

$$Z(x_1,x_2) \approx \frac{x_1^2+x_2^2}{2R}. \quad [S2]$$

Deformations from this initial state are quantified via a local normal displacement $f(x_1,x_2)$ perpendicular to the undeformed surface and tangential displacements $u_1(x_1,x_2)$ and $u_2(x_1,x_2)$ within the shell along the projections of the x_1 and x_2 axes on the sphere, respectively. In terms of these fields, a point $(x_1,x_2,Z(x_1,x_2))$ in the undeformed state moves to $(x_1+u_1-f\partial_1 Z, x_2+u_2-f\partial_2 Z, Z+f)$ to lowest order in the slopes $\partial_i Z = x_i/R$. The strain tensor is defined by the relation between the length ds' of a line element in the deformed state and the corresponding line element length ds in the undeformed state (2):

$$(ds')^2 = ds^2 + 2u_{ij}dx_i dx_j. \quad [S3]$$

With this definition and neglecting terms of order $(\partial_i Z)^2$ and their derivatives, we find the nonlinear strain tensor used in the main text,

$$u_{ij}(\mathbf{x}) = \frac{1}{2}\left(\partial_i u_j + \partial_j u_i + \partial_i f \partial_j f\right) - \delta_{ij}\frac{f}{R}. \quad [S4]$$

The stretching energy is then given by (2)

$$G_s = \frac{1}{2}\int dS\left[2\mu u_{ij}^2 + \lambda u_{kk}^2\right], \quad [S5]$$

where μ and λ are the Lamé coefficients and dS is an area element.

We also include a bending energy of the Helfrich form (3) that penalizes changes in local curvature,

$$G_b = \frac{\kappa}{2}\int dS(H-H_0)^2, \quad [S6]$$

where κ is the bending rigidity, H is the mean curvature, and H_0 is the spontaneous mean curvature (which we take to be equal everywhere to the curvature $2/R$ of the undeformed shell). For a shallow section of the shell, the local curvature can be written in terms of the height field $Z(x_1,x_2)+f(x_1,x_2)$ as

$$H = \nabla^2(Z+f) = \frac{2}{R} + \nabla^2 f, \quad [S7]$$

where $\nabla^2 = \partial_{11} + \partial_{22}$ is the Laplacian in the tangential coordinate system. Finally, the energy due to an external pressure p equals the work done,

$$W = -p\int dS\, f. \quad [S8]$$

The area element is $dS = dx_1 dx_2/\sqrt{1-(x_1^2+x_2^2)/R^2} \approx dx_1 dx_2$ when terms of order $(x_i/R)^2$ and above are neglected. Summing the stretching, bending, and pressure energies leads to the elastic energy expression $G = G_s + G_b + W$, Eq. **1** in the main text.

Because we are restricted to a shallow section of the shell, the theory is strictly applicable only to deformations whose length scale is small compared with the radius R. The typical length scale ℓ of deformations can be obtained by balancing the bending and stretching energies G_b and G_s discussed above. Upon noting that the stretching free-energy density in a region of size ℓ is $\mathcal{G}_s \sim Y(f/R)^2$, where Y is a typical elastic constant, and $\mathcal{G}_b \sim \kappa f^2/\ell^4$, we recover the Föppl–von Kármán length scale introduced in the main text,

$$\ell^* = \frac{R}{\gamma^{1/4}}, \quad [S9]$$

where the Föppl–von Kármán number is $\gamma = YR^2/\kappa$. More sophisticated calculations (sketched below) show that the relevant elastic constant is the 2D Young's modulus, $Y = 4\mu(\mu+\lambda)/(2\mu+\lambda)$.

For a shell made up of an elastic material of thickness h, taking Y and κ from the 3D Young's modulus of an isotropic solid within thin shell theory provides the estimate $\gamma \approx 10(R/h)^2$ (2). For shallow shell theory to be valid, we need $\ell^* \ll R$. Hence shallow shell theory is valid when $\gamma \gg 1$, i.e., $R \gg h$, which is precisely the limit of large, thin curved shells that are most susceptible to thermal fluctuations. This agreement between shallow shell theory and more general shell theories that are applicable over entire spherical shells has been discussed by Koiter (4) in the context of the response of a shell to a point force at its poles. Shallow shell theory was also used to study the stability of pressurized shells by Hutchinson (5). In both cases, shallow shell theory was shown to be valid for thin shells such that $h/R \ll 1$. Because thermal fluctuations are relevant only for shells with radii several orders of magnitude larger than their thickness, shallow shell theory is an excellent starting point for the extremely thin shells of interest to us here.

Elimination of in-Plane Phonon Modes and Uniform Spherical Contraction by Gaussian Integration. A spherical shell under the action of a uniform external pressure that is lower than the critical buckling threshold responds by contracting uniformly by an amount f_0. The out-of-plane deformation field can then be written as a sum of its uniform and nonuniform parts,

$$f(\mathbf{x}) = f_0 + f'(\mathbf{x}) = f_0 + \sum_{\mathbf{q}\neq 0} f_{\mathbf{q}} e^{-i\mathbf{q}\cdot\mathbf{x}}, \qquad \textbf{[S10]}$$

where $f'(\mathbf{x})$ represents the contribution to the field from its $\mathbf{q}\neq 0$ Fourier components. (In this section, for ease of presentation we use the normalization $f_{\mathbf{q}} \equiv \frac{1}{A}\int d^2x\, f(\mathbf{x}) e^{i\mathbf{q}\cdot\mathbf{x}}$, where A is the area of integration in the (x_1,x_2) plane. The inverse transform is then $f(\mathbf{x}) = \sum_{\mathbf{q}} f_{\mathbf{q}} e^{-i\mathbf{q}\cdot\mathbf{x}}$.) With this decomposition, $\int d^2x\, f'(\mathbf{x}) = 0$ and thus only f_0 contributes to the pressure work W. On the other hand, only f' contributes to the nonlinear part of the strain tensor. Hence the elastic energy $G = G_b + G_s + W$ defined above is harmonic in the in-plane phonon fields $u_1(\mathbf{x})$ and $u_2(\mathbf{x})$ as well as in the uniform contraction f_0. To analyze the effects of anharmonicity, it is useful to eliminate these fields and define an effective free energy (6),

$$G_{\text{eff}}[f'] = -k_{\text{B}}T \ln\left\{\int \mathcal{D}\vec{u}(x_1,x_2)\int df_0 e^{-G[f',f_0,u_1,u_2]/k_{\text{B}}T}\right\}. \qquad \textbf{[S11]}$$

To carry out the functional integrals in Eq. **S11** for a fixed out-of-plane displacement field $f'(\mathbf{x})$, the strain tensor u_{ij} must also be separated into its $\mathbf{q}=0$ and $\mathbf{q}\neq 0$ components,

$$u_{ij} = \tilde{u}^0_{ij} + \sum_{\mathbf{q}\neq 0}\left[\frac{i}{2}\left(q_i u_j(\mathbf{q}) + q_j u_i(\mathbf{q})\right) + A_{ij}(\mathbf{q}) - \delta_{ij}\frac{f_{\mathbf{q}}}{R}\right] e^{-i\mathbf{q}\cdot\mathbf{x}}, \qquad \textbf{[S12]}$$

where

$$A_{ij}(\mathbf{q}) = \frac{1}{2A}\int d^2x\, \partial_i f' \partial_j f' e^{i\mathbf{q}\cdot\mathbf{x}}. \qquad \textbf{[S13]}$$

The uniform part of the strain tensor has the following components:

$$\begin{aligned} \tilde{u}^0_{11} &= u^0_{11} + A_{11}(\mathbf{0}) - \frac{f_0}{R}, \\ \tilde{u}^0_{22} &= u^0_{22} + A_{22}(\mathbf{0}) - \frac{f_0}{R}, \\ \tilde{u}^0_{12} &= u^0_{12} + A_{12}(\mathbf{0}). \end{aligned} \qquad \textbf{[S14]}$$

Here, u^0_{ij} are the uniform in-plane strains that are independent of f_0. This restriction implies that $u^0_{11} + u^0_{22} = 0$ because a simultaneous uniform in-plane strain of the same sign in the x_1 and x_2 directions corresponds to a change in radius of the sphere and thus cannot be decoupled from f_0. Hence in addition to f_0 and u^0_{12}, there is only one more independent degree of freedom, $\Delta u^0 \equiv u^0_{11} - u^0_{22}$, that determines the uniform contribution to the strain tensor.

Finally we perform the functional integration in Eq. **S11** over the phonon fields u_i as well as the three independent contributions to the uniform part of the strain tensor: f_0, $\tilde{u}^0_{12}$, and Δu^0. The resulting effective free energy is, upon suppressing an additive constant,

$$\begin{aligned} G_{\text{eff}} = \int d^2x \left[\frac{\kappa}{2}\left(\nabla^2 f'\right)^2 + \frac{Y}{2}\left(\frac{1}{2}P^{\text{T}}_{ij}\partial_i f' \partial_j f' - \frac{f'}{R}\right)^2\right] \\ - A\frac{pR}{2}\left[A_{11}(\mathbf{0}) + A_{22}(\mathbf{0})\right], \end{aligned} \qquad \textbf{[S15]}$$

where $P^{\text{T}}_{ij} = \delta_{ij} - \partial_i\partial_j/\nabla^2$ is the transverse projection operator. Note that as a result of the integration the Lamé coefficients μ and λ enter only through the 2D Young's modulus $Y = 4\mu(\mu+\lambda)/(2\mu+\lambda)$. Finally, substituting

$$A_{11}(\mathbf{0}) + A_{22}(\mathbf{0}) = \frac{1}{2A}\int d^2x\left[(\partial_1 f')^2 + (\partial_2 f')^2\right] = \frac{1}{2A}\int d^2x |\nabla f'|^2 \qquad \textbf{[S16]}$$

in Eq. **S15** gives the effective free energy used in the analysis, Eq. **3** in the main text. In the following, we drop the prime on the out-of-plane displacement field because f_0 has now been eliminated. When only the harmonic contributions are considered, the equipartition result for the thermally generated Fourier components $f_{\mathbf{q}} = \int d^2x\, f(\mathbf{x})\exp(i\mathbf{q}\cdot\mathbf{x})$ with 2D wavevector $\mathbf{q}$ are

$$\left\langle f_{\mathbf{q}} f_{\mathbf{q}'}\right\rangle_0 = \frac{Ak_{\text{B}}T\delta_{\mathbf{q},-\mathbf{q}'}}{\kappa q^4 - \frac{pR}{2}q^2 + \frac{Y}{R^2}}, \qquad \textbf{[S17]}$$

where A is the area of integration in the (x_1,x_2) plane. This harmonic spectrum (Eq. **4** in the main text) takes on corrections due to the anharmonic terms that are calculated in the next section.

One-Loop Contributions to the Self-Energy. Here we describe the self-energy used to calculate the leading anharmonic corrections to the fluctuation spectrum in the main text. The Feynman rules obtained from the effective free energy $G_{\text{eff}}[f]$ are summarized in Fig. S2. Henceforth, Fourier components are defined as in the main text: $f_{\mathbf{q}} = \int d^2x\, f(\mathbf{x})\exp(i\mathbf{q}\cdot\mathbf{x})$ with 2D wavevector $\mathbf{q}$. The inverse Fourier transformation of the out-of-plane deformation field is

$$f(\mathbf{x}) = \frac{1}{A}\sum_{\mathbf{q}\neq 0} f_{\mathbf{q}} e^{-i\mathbf{q}\cdot\mathbf{x}}, \qquad \textbf{[S18]}$$

where A is the area of integration in the (x_1,x_2) plane and the sum is over all allowed Fourier modes. The one-loop contributions to the self-energy $\Sigma(\mathbf{q})$ due to the anharmonic three-point vertex (cubic term in the energy) and the four-point vertex (quartic term) are summarized in Fig. S3. Fig. S3*A* is also present in the calculation for flat membranes (6) and provides a contribution

$$-Y\int \frac{d^2k}{(2\pi)^2}\frac{\left[P^{\text{T}}_{ij}(\mathbf{k})q_i q_j\right]^2}{\kappa|\mathbf{q}+\mathbf{k}|^4 - \frac{pR}{2}|\mathbf{q}+\mathbf{k}|^2 + \frac{Y}{R^2}} \qquad \textbf{[S19]}$$

to the self-energy. Fig. S3*B* involves two-vertex terms arising from the cubic coupling unique to shells with curvature (note that, despite "amputation" of the propagator legs, the diagrams are distinct because the slashes decide the momentum terms that survive various index contractions in addition to determining the momentum of the transverse projection operator introduced at each vertex). The net contribution to the self-energy from the four diagrams in Fig. S3*B* is

$$\begin{aligned} &\frac{Y^2}{R^2}\int \frac{d^2k}{(2\pi)^2}\frac{1}{\left(\kappa|\mathbf{q}+\mathbf{k}|^4 - \frac{pR}{2}|\mathbf{q}+\mathbf{k}|^2 + \frac{Y}{R^2}\right)\left(\kappa k^4 - \frac{pR}{2}k^2 + \frac{Y}{R^2}\right)} \\ &\times\left\{\frac{1}{2}\left[P^{\text{T}}_{ij}(\mathbf{q})k_i k_j\right]^2 + \left[P^{\text{T}}_{ij}(\mathbf{k})q_i q_j\right]^2 + \left[P^{\text{T}}_{ij}(\mathbf{k})q_i q_j\right]\left[P^{\text{T}}_{lm}(\mathbf{k}+\mathbf{q})q_l q_m\right]\right. \\ &\left. + 2\left[P^{\text{T}}_{ij}(\mathbf{k})q_i q_j\right]\left[P^{\text{T}}_{lm}(\mathbf{q})k_l k_m\right]\right\}. \end{aligned} \qquad \textbf{[S20]}$$

Whereas the inverse of the harmonic correlation function, Eq. **S17**, contains only terms of order q^0, q^2, q^4, the one-loop corrections to the spectrum (Eqs. **S19** and **S20**) generate terms with

these powers of q as well as terms of order q^6 and above in the full inverse fluctuation spectrum. If we keep only terms of order q^4 and below in the calculation of the one-loop fluctuation spectrum, we can provide an approximate description of the low-q behavior of the shell in terms of effective elastic constants,

$$Ak_BT\left\langle |f_{\mathbf{q}\to\mathbf{0}}|^2\right\rangle^{-1} \equiv \kappa_R q^4 - \frac{p_R R}{2}q^2 + \frac{Y_R}{R^2} + O(q^6), \qquad \textbf{[S21]}$$

where Y_R, κ_R, and p_R are the effective Young's modulus, bending rigidity, and dimensionless pressure, respectively. At long length scales, probes of the elastic properties of thermally fluctuating shells would provide information of these effective elastic constants rather than the "bare" constants Y, κ, and p that describe the zero-temperature shell. Upon expanding the integrands in Eqs. **S19** and **S20** to the self-energy to $O(q^4)$, the momentum integrals can be carried out analytically to obtain

$$Y_R = Y\left[1 - \frac{3}{128\pi}\frac{k_BT}{\kappa}\frac{\sqrt{\gamma}}{(1-\eta^2)^{3/2}}\left(\eta\sqrt{1-\eta^2} + \pi - \cos^{-1}\eta\right)\right], \qquad \textbf{[S22]}$$

$$\kappa_R = \kappa\left[1 + \frac{1}{30,720\pi}\frac{k_BT}{\kappa}\frac{\sqrt{\gamma}}{(1-\eta^2)^{7/2}} \times\left[\eta\sqrt{1-\eta^2}\left(-1,699 + 3,758\eta^2 - 2,104\eta^4\right)\right.\right.$$
$$\left.\left. +15\left(61 - 288\eta^2 + 416\eta^4 - 192\eta^6\right)\left(\pi - \cos^{-1}\eta\right)\right]\right], \qquad \textbf{[S23]}$$

$$\eta_R = \eta + \frac{1}{1,536\pi}\frac{k_BT}{\kappa}\frac{\sqrt{\gamma}}{(1-\eta^2)^{5/2}} \times\left[\sqrt{1-\eta^2}\left(64 - 67\eta^2\right) + 3\left(21\eta - 22\eta^3\right)\left(\pi - \cos^{-1}\eta\right)\right], \qquad \textbf{[S24]}$$

where we have defined a dimensionless pressure $\eta \equiv p/p_c$ and $p_c = 4\sqrt{\kappa Y}/R^2$ is the classical buckling pressure of the shell. We see explicitly that the quantities diverge in the limit $\eta \to 1$. To lowest order in the external pressure, we have

$$Y_R \approx Y\left[1 - \frac{3}{256}\frac{k_BT}{\kappa}\sqrt{\gamma}\left(1 + \frac{4}{\pi}\frac{p}{p_c}\right)\right], \qquad \textbf{[S25]}$$

$$p_R \approx p + \frac{1}{24\pi}\frac{k_BT}{\kappa}p_c\sqrt{\gamma}\left(1 + \frac{63\pi}{128}\frac{p}{p_c}\right), \qquad \textbf{[S26]}$$

and

$$\kappa_R \approx \kappa\left[1 + \frac{61}{4,096}\frac{k_BT}{\kappa}\sqrt{\gamma}\left(1 - \frac{1,568}{915\pi}\frac{p}{p_c}\right)\right]. \qquad \textbf{[S27]}$$

These are the approximate renormalized elastic quantities tabulated in Eqs. **7**–**9** in the main text.

In evaluating the above expressions, the momentum integrals in Eqs. **S19**–**S20** must strictly speaking be carried out over the phase space of all allowed Fourier modes $f(\mathbf{k})$ of the system, which go from some low-k cutoff $k_{min}\sim 1/R$ to a high-k cutoff set by the microscopic lattice constant. However, because all integrals converge in the UV limit $k \to \infty$, the upper limit of the k-integrals can be extended to ∞. The integrals are well behaved at low momenta due to the mass term $\sim Y/R^2$ in the propagator. Hence we carry out the momentum integrals over the entire 2D plane of $\mathbf{k}$. The excess contribution to the self-energy by including spurious Fourier modes with $0 < k < 1/R$, i.e., for wave vectors less than the natural infrared cutoff $k_{min}\sim 1/R$, gives rise to an error of roughly $1/\sqrt{\gamma}$, which is negligible for extremely thin shells. This correction is of similar magnitude to the errors introduced by using shallow shell theory (which is inaccurate for the longest-wavelength modes with wave vector $k \sim 1/R$), which are also negligible in the thin-shell limit.

Calculation of Fluctuation Spectrum with Spherical Harmonics. Whereas the perturbation theory calculations were carried out using a basis of Fourier modes in a shallow section of the shell to decompose the radial displacement field, the fluctuation spectrum is most efficiently measured in simulations using a spherical harmonics expansion. To compare the simulation results to the expected corrections from perturbation theory, we use the description of the shell in terms of the effective elastic constants Y_R, κ_R, and p_R, Eqs. **7**–**9** in the main text.

Consider a spherical shell of radius R with bending rigidity κ and Lamé coefficients λ and μ, experiencing a tangential displacement field $\mathbf{u} = (u_x, u_y)$ and a radial displacement field f. Like any smooth vector field, $\mathbf{u}$ can be decomposed into an irrotational (curl-free) part and a solenoidal (divergence-free) part, $\mathbf{u} \equiv \nabla\Psi + \mathbf{v}$, where the scalar function Ψ generates the irrotational component and $\mathbf{v}$ is the solenoidal component. Upon expanding $f \equiv \sum_{l,m} A_{lm} R Y_l^m$ and $\Psi \equiv \sum_{l,m} B_{lm} R^2 Y_l^m$ in terms of spherical harmonics $Y_l^m(\theta,\phi)$, the elastic energy of the deformation to quadratic order in the fields is given by (7)

$$G = R^2\sum_{l,m}\left\{\left[\frac{\kappa}{2}\frac{(l+2)^2(l-1)^2}{R^2} + 2K\right]A_{lm}^2 - 2Kl(l+1)A_{lm}B_{lm}\right\} + \frac{1}{2}l(l+1)\left[(K+\mu)l(l+1) - 2\mu\right]B_{lm}^2\Big\} + G_{sol}(\mathbf{v}), \qquad \textbf{[S28]}$$

where $K = \lambda + \mu$ is the bulk modulus. The solenoidal component $\mathbf{v}$ does not couple to the radial displacement field and provides an independent contribution G_{sol} that is purely quadratic in the field $\mathbf{v}$.

To this elastic energy, we also add the surface energy-like contribution $G_S = -(pR/2)\Delta A$ due to the "negative surface tension" $-pR/2$ present in the shell when it is uniformly compressed in response to an external pressure p. Here ΔA is the excess area due to deformations about the average radius. In terms of spherical harmonic coefficients, this area change can be written (8)

$$\Delta A \approx R^2\sum_{l>1,m} A_{lm}^2\left[1 + \frac{l(l+1)}{2}\right]. \qquad \textbf{[S29]}$$

As we did for the elastic energy in shallow shell theory, we can now integrate out the quadratic fluctuating quantities B_{lm} and the solenoidal field $\mathbf{v}$ to obtain an effective free energy in terms of the radial displacements alone:

$$G_{eff} = \frac{R^2}{2}\sum_{l>1,m}\left\{\frac{\kappa(l+2)^2(l-1)^2}{R^2} - pR\left[1 + \frac{l(l+1)}{2}\right] + \frac{4\mu(\mu+\lambda)\left(l^2+l-2\right)}{(2\mu+\lambda)(l^2+l) - 2\mu}\right\}A_{lm}^2. \qquad \textbf{[S30]}$$

The fluctuation amplitude is obtained via the equipartition theorem

$$\begin{aligned} k_B T\left\langle |A_{lm}|^2\right\rangle_0^{-1} &= \kappa(l+2)^2(l-1)^2 - pR^3\left[1+\frac{l(l+1)}{2}\right] \\ &\quad + \frac{4\mu(\mu+\lambda)(l^2+l+2)}{(2\mu+\lambda)(l^2+l)-2\mu}R^2 \\ &= \kappa(l+2)^2(l-1)^2 - pR^3\left[1+\frac{l(l+1)}{2}\right] \\ &\quad + \frac{Y}{1+\frac{Y}{2\mu(l^2+l-2)}}R^2, \end{aligned} \qquad \text{[S31]}$$

where $Y = 4\mu(\mu+\lambda)/(2\mu+\lambda)$ is the 2D Young's modulus introduced earlier. The effect of anharmonic contributions to the fluctuation spectrum can now be calculated by using the effective temperature-dependent quantities Y_R, κ_R, and p_R in place of the bare elastic constants in the above expression. However, the last term in Eq. **S31** also requires knowledge of the thermal corrections to the Lamé coefficient μ that was eliminated in the shallow shell calculation when the tangential displacement fields were integrated out. For the discretized stretching energy used in the simulations, we have $\mu = 3Y/8$. If we assume that this relationship is not significantly changed by the anharmonic corrections to one-loop order, then $\mu_R \approx 3Y_R/8$. Upon substituting this approximation together with the other effective elastic parameters in Eq. **S31**, we find

$$\begin{aligned} k_B T\left\langle |A_{lm}|^2\right\rangle^{-1} &\approx \kappa_R(l+2)^2(l-1)^2 - p_R R^3\left[1+\frac{l(l+1)}{2}\right] \\ &\quad + Y_R R^2\left[\frac{3(l^2+l-2)}{3(l^2+l)-2}\right], \end{aligned} \qquad \text{[S32]}$$

which is the same as as Eq. **11** in the main text. {If, as is more likely, the thermal corrections to μ and Y do differ to $O(k_BT)$, we can nevertheless estimate that the resulting error term introduced by the assumption $\mu_R \approx 3Y_R/8$ is suppressed by a factor $4/[3(l^2+l-2)+4]$ relative to the anharmonic corrections and is thus at least an order of magnitude smaller than the anharmonic contribution itself when $l > 1$.}

Linear Response of the Shell to Point Forces. We calculate the response of the shallow shell to a point force at the origin, corresponding to a force field $h(\mathbf{x}) = F\delta^2(\mathbf{x})$. The Fourier decomposition of this force field is

$$h_{\mathbf{q}} = F, \quad \text{for all } \mathbf{q}. \qquad \text{[S33]}$$

The linear response of the deformation field f to this force is related to its fluctuation amplitudes in the absence of the force, $\langle |f_{\mathbf{q}}|^2\rangle_{h=0}$, by the fluctuation-response theorem

$$\langle f_{\mathbf{q}}\rangle = \frac{\left\langle |f_{\mathbf{q}}|^2\right\rangle_{h=0}}{Ak_BT}h_{\mathbf{q}} = \frac{\left\langle |f_{\mathbf{q}}|^2\right\rangle_{h=0}}{Ak_BT}F. \qquad \text{[S34]}$$

The inward deflection at the origin is then

$$\langle f(\mathbf{x}=0)\rangle = \frac{1}{A}\sum_{\mathbf{q}}\langle f_{\mathbf{q}}\rangle = \frac{F}{A^2k_BT}\sum_{\mathbf{q}}\left\langle |f_{\mathbf{q}}|^2\right\rangle_{h=0}. \qquad \text{[S35]}$$

This can be related to $\langle f^2\rangle$, the mean square fluctuations of the deformation field in real space, which is a position-independent quantity in the absence of nonuniform external forces:

$$\begin{aligned} \langle f^2\rangle \equiv \left\langle [f(\mathbf{x})]^2\right\rangle_{h=0} &= \frac{1}{A^2}\sum_{\mathbf{q}}\sum_{\mathbf{q}'}\left\langle f_{\mathbf{q}}f_{\mathbf{q}'}\right\rangle e^{-i(\mathbf{q}+\mathbf{q}')\cdot\mathbf{x}} \\ &= \frac{1}{A^2}\sum_{\mathbf{q}}\left\langle |f_{\mathbf{q}}|^2\right\rangle_{h=0}. \end{aligned} \qquad \text{[S36]}$$

From Eqs. **S35** and **S36**, we obtain

$$\langle f(\mathbf{x}=0)\rangle = \frac{F}{k_BT}\langle f^2\rangle. \qquad \text{[S37]}$$

This equation relates the depth of the indentation due to a force F at the origin to the mean square fluctuations of the deformation field f in the absence of such a force.

When only harmonic contributions are considered, Eq. **S17** gives us the mean square amplitude $\langle |f_{\mathbf{q}}|^2\rangle_0 = Ak_BT/(\kappa q^4 - pRq^2/2 + Y/R^2)$ in terms of the elastic constants and external pressure. Upon taking the continuum limit of the sum over wave vectors $\sum_{\mathbf{q}} \to A\int d^2q/(2\pi)^2$, we can calculate the fluctuation amplitudes exactly,

$$\langle f^2\rangle = \int \frac{d^2q}{(2\pi)^2}\frac{k_BT}{\kappa q^4 - \frac{pR}{2}q^2 + \frac{Y}{R^2}} = \frac{Rk_BT}{8\sqrt{\kappa Y}}\frac{1+\frac{2}{\pi}\sin^{-1}\eta}{\sqrt{1-\eta^2}}, \qquad \text{[S38]}$$

where $\eta = p/p_c = pR^2/(4\sqrt{\kappa Y})$ is the dimensionless pressure, and $\eta < 1$; i.e., we restrict ourselves to pressures below the classical buckling pressure. From Eqs. **S37** and **S38**, we get the linear relation between the indentation force and the depth of the resulting deformation:

$$F = \frac{8\sqrt{\kappa Y}}{R}\frac{\sqrt{1-\eta^2}}{1+\frac{2}{\pi}\sin^{-1}\eta}\langle f(\mathbf{x}=0)\rangle. \qquad \text{[S39]}$$

The temperature drops out and we obtain a result valid for $T = 0$ shells as well. The expression reproduces the well-known Reissner solution (9) for the linear response of a spherical shell to a point force when $\eta = 0$ and also reproduces the recent result from Vella et al. (10) for indentations on spherical shells with an internal pressure when $\eta < 1$. At finite temperatures, however, anharmonic effects contribute terms of order $(k_BT)^2$ and higher to $\langle f^2\rangle$, making the response temperature dependent.

In the simulations, the shells contract by a small amount due to thermal fluctuations, even in the absence of external forces. Thus, indentations are measured relative to the thermally averaged pole-to-pole distance of the shell at finite temperature, $\langle z_0\rangle < 2R$. Equal and opposite inward forces are applied to the north and south poles of the shell to maintain a force balance (details in *Materials and Methods* in the main text) and the resulting average pole-to-pole distance, $\langle z\rangle$, is measured. This corresponds to an average indentation depth of $(\langle z_0\rangle - \langle z\rangle)/2$ at each pole, with associated force (from Eq. **S37**)

$$F = \frac{k_BT}{\langle f^2\rangle}\frac{(\langle z_0\rangle - \langle z\rangle)}{2} \equiv k_s(\langle z_0\rangle - \langle z\rangle); \qquad \text{[S40]}$$

i.e., the shell as a whole acts as a spring with spring constant

$$k_s = \frac{k_BT}{2\langle f^2\rangle}. \qquad \text{[S41]}$$

At $T = 0$, we have

$$k_s = \frac{4\sqrt{\kappa Y}}{R}\frac{\sqrt{1-\eta^2}}{1+\frac{2}{\pi}\sin^{-1}\eta}; \qquad \textbf{[S42]}$$

in particular, $k_s = 4\sqrt{\kappa Y}/R$ in the absence of external pressure. Anharmonic contributions change the fluctuation amplitude $\langle f^2\rangle$ and hence the linear response. To lowest order in temperature, the effects of anharmonic contributions can be obtained by using the renormalized elastic constants calculated using perturbation theory (Eqs. **S25**–**S27**) in Eq. **S42** and keeping terms to $O(T)$. In particular, even if the bare pressure $p = 0$, the renormalized dimensionless pressure p_R is nonzero and affects the spring constant, as do the temperature-dependent effective elastic moduli. The result in this case is

$$k_s(T>0) \approx \frac{4\sqrt{\kappa Y}}{R}\left[1 - 0.0069\frac{k_B T}{\kappa}\sqrt{\gamma}\right]. \qquad \textbf{[S43]}$$

This is the theoretical prediction quoted as Eq. **13** in the main text.

Measuring the Effective Spring Constant from Monte Carlo Simulations. We extract the spring constants of thermally fluctuating shells for Fig. 3*C* in the main text by using the relation between k_s and fluctuations in the transverse displacement field f (Eq. **S41**). It is straightforward to measure the average pole-to-pole distance of the fluctuating shell in the absence of external forces, $\langle z_0\rangle = \langle R - f_N - f_S\rangle$, where f_N and f_S are the inward displacements at the north and south poles, respectively. Because the displacements at the poles are expected to be independent of each other, the mean squared fluctuations in z_0 are closely related to the mean square fluctuations in f:

$$\langle z_0^2\rangle - \langle z_0\rangle^2 \approx 2\langle f^2\rangle. \qquad \textbf{[S44]}$$

The spring constant can thus be measured indirectly from the fluctuations in the pole-to-pole distance, using Eq. **S41**:

$$k_s = \frac{k_B T}{2\langle f^2\rangle} \approx \frac{k_B T}{\langle z_0^2\rangle - \langle z_0\rangle^2}. \qquad \textbf{[S45]}$$

1. van der Heijden AMA (2009) *W. T. Koiter's Elastic Stability of Solids and Structures* (Lecture notes compiled by the author) (Cambridge Univ Press, Cambridge, UK).
2. Landau L, Lifshitz E (1986) *Theory of Elasticity* (Butterworth-Heinemann, Boston), 3rd Ed.
3. Helfrich W (1973) Elastic properties of lipid bilayers: Theory and possible experiments. *Z Naturforsch C* 28(11):693–703.
4. Koiter W (1963) *Progress in Applied Mechanics*, The Prager Anniversary Volume (MacMillan, New York), pp 155–169.
5. Hutchinson J (1967) Imperfection sensitivity of externally pressurized spherical shells. *J Appl Mech* 34:49–55.
6. Nelson DR (2004) Theory of the crumpling transition. *Statistical Mechanics of Membranes and Surfaces*, eds Nelson DR, Piran T, Weinberg S (World Scientific, Singapore), 2nd Ed, pp 131–148.
7. Zhang Z, Davis HT, Kroll DM (1993) Scaling behavior of self-avoiding tethered vesicles. *Phys Rev E Stat Phys Plasmas Fluids Relat Interdiscip Topics* 48(2):R651–R654.
8. Milner ST, Safran SA (1987) Dynamical fluctuations of droplet microemulsions and vesicles. *Phys Rev A* 36(9):4371–4379.
9. Reissner E (1946) Stresses and small displacements of shallow spherical shells. I. *J Math Phys* 25:80–85.
10. Vella D, Ajdari A, Vaziri A, Boudaoud A (2012) The indentation of pressurized elastic shells: From polymeric capsules to yeast cells. *J R Soc Interface* 9(68):448–455.

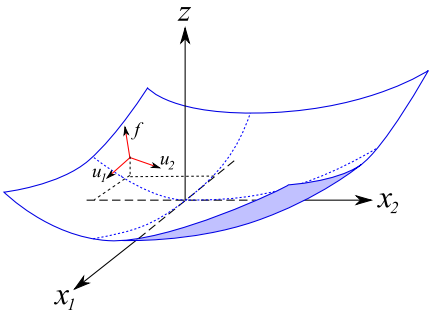

Fig. S1. The coordinate system in shallow shell theory. A section of the undeformed sphere is shown with the (x_1, x_2) plane tangential to it at the origin. The red arrows show the directions into which displacements $u_1(x_1, x_2)$, $u_2(x_1, x_2)$, and $f(x_1, x_2)$ are decomposed at a particular point in the coordinate plane.

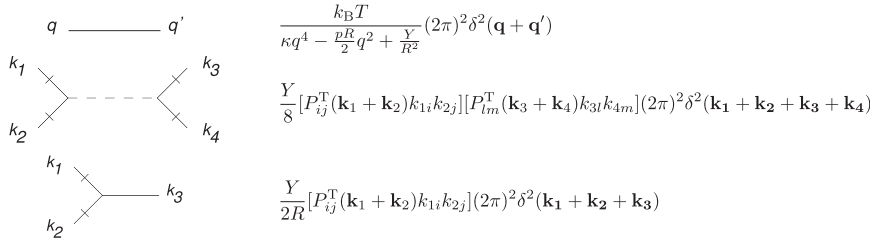

Fig. S2. The bare propagator for f_q and the vertices arising from the nonquadratic terms in G_{eff}. The slashes on specific legs denote spatial derivatives. $P^T_{ij}(\mathbf{q}) = \delta_{ij} - q_i q_j/q^2$ is the transverse projection operator in momentum space. Note an unusual feature of this graphical perturbation theory: The system size, i.e., the sphere radius R, enters explicitly both in the propagator and as a coupling constant in the third-order interaction vertex.

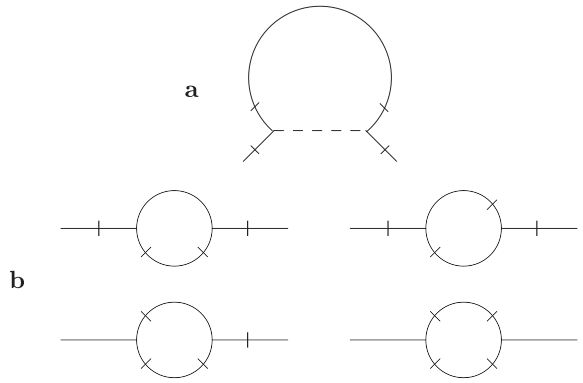

Fig. S3. One-loop corrections to the two-point height–height correlation function in momentum space. Note that in calculating the self-energy, the external propagators are not included; i.e., they are "amputated." The contribution in *A* resembles that for membranes with a flat ground state, except for the *R*-dependent pressure and mass terms in the propagator. The nonlinear corrections in *B*, however, arise from a cubic coupling constant proportional to $1/R$ and are unique to the spherical geometry.

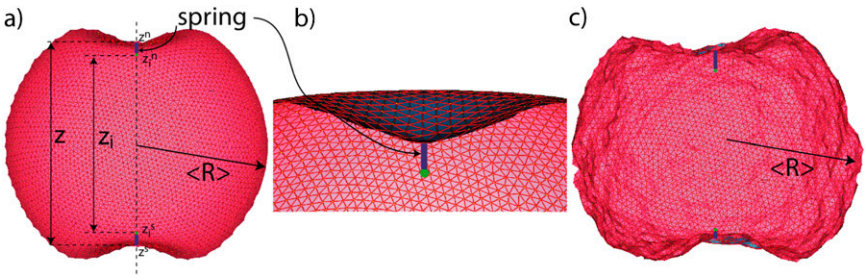

Fig. S4. Illustration of the indentation simulation of a randomly triangulated shell. Shown here are vertical cuts through a shell of radius $R_0 = 20\ r_0$ at dimensionless temperature $k_B T\sqrt{\gamma}/\kappa = 10^{-5}$ (*A* and *B*) and $k_B T\sqrt{\gamma}/\kappa = 15$ (*C*). A shell at low temperature (*A*) is indented by two harmonic springs (dark blue lines) attached to the north (z^N) and south (z^S) poles of the shell. Fixing the springs at a separation $z_i = z_i^N - z_i^S$ leads to a pole separation z. The green points indicate the positions z_i^N and z_i^S of the fixed end points of the springs. (*B*) A close-up of the north pole of the shell displayed in *A*. The configuration contains a minority of five- and sevenfold coordinated vertices in addition to sixfold coordinated ones. (*C*) Illustration of a fluctuating shell at $R_0 = 20\ r_0$ and $k_B T\sqrt{\gamma}/\kappa = 10^{-5}$.